IFSCC 2025 full paper (IFSCC2025-1514)

Linking Visible Features of Facial Aging to Multimodal Instrumental Measurements Using Advanced Chemometrics: A Comprehensive Multi-Ethnic Study in Healthy Women

Ali ASSI[1,*], Guénolé GRIGNON[1], Raoul MISSODEY[1], Colombe LOPEZ[2], Agnes PIGNOL-LAVOIX[3], Meryem NILI[3], Samuel RALAMBONDRAINY[1], Jean-Hubert CAUCHARD[1], Rodolphe KORICHI[1], Franck BONNIER[1]

[1]In Vivo Efficacy Platform, LVMH Recherche, Saint Jean De Braye; [2]DAMAE Medical, Paris; [3]COMPLIFE France, Lyon, France

1. Introduction

Skin aging is a gradual, multifactorial process influenced by intrinsic factors like genetics and hormones, and extrinsic factors including UV radiation, pollution, and lifestyle choices. These contribute to visible signs of aging such as wrinkles, loss of firmness, and pigmentation irregularities [1,2]. Clinical scoring, performed by dermatologists and trained experts, quantifies the visible signs of aging through visual inspection or palpation, utilizing standardized scoring systems. Notable examples include the Skin Aging Atlas [3–5], which provides a comprehensive visual grading system with photographic references, and the SCINEXA scale [6], which combines multiple visible features. While clinical evaluations are practical, instrumental measurements enhance accuracy and objectivity by providing quantitative parameters [7,8]. These measurements offer a more precise and less subjective assessment of skin aging. Dicanio et al. introduced the Calculated Age Score (CAS) combining clinical and instrumental data [9]. Studies increasingly adopt multimodal approaches, combining clinical scoring, instrumental metrics, and biochemical parameters. Multivariate tools for analyzing these variables are rarely discussed concerning aging effects. Nkengne et al. used Principal Component Analysis (PCA) to create a skin aging index based on facial attributes [10]. This approach was further developed by He et al. [11] and Pardo et al. [12], who included instrumental measurements. Recently, Robic et al. proposed a global model of skin aging indices, integrating clinical scores, image analysis, and assessments of elastic properties [13].

Among all the techniques deployed to construct models and projections, photography is preferred for accessing visible features of aging. However, confocal imaging provides valuable information about the underlying microstructures within the skin layers [14], notably, to study the several modifications involved in skin aging process. Histologically, the epidermis becomes thinner, and the dermis experiences a reduction in extracellular matrix components, leading to a loss of skin elasticity and firmness [15]. Collagen fibers become fragmented and disorganized, while elastin fibers lose their elasticity and integrity [16]. At the cellular level,

keratinocytes, the primary cells in the epidermis, exhibit reduced proliferation and increased senescence [17]. Fibroblasts in the dermis, responsible for producing collagen and elastin, also show diminished activity, with an accumulation of damaged or senescent cells, contributing to the thinning and fragility of the skin [18]. Cellular and histological effects of aging are well-evidenced in vitro and ex vivo, but in vivo observation is challenging due to limitations of non-invasive imaging. Nevertheless, techniques like High-Frequency Ultrasound (HFUS) imaging, which assesses dermal thickness, density, and integrity, are established for highlighting aging effects [19]. Notably, the SELEB (Sub-Epidermal Low Echogenic Band) is a well-established echogenic marker of aging that has been studied in various populations [20].

Reflectance Confocal Microscopy (RCM) is a well-established method for characterizing skin in vivo at cellular resolution. It assesses aging effects through grading criteria like furrow patterns, furrow width, cellular atypia, and collagen characteristics [21]. Computational methods for image analysis and automated feature extraction have strengthened RCM's position as a reference tool [22]. MultiPhoton Microscopy (MPM) and Line-Field Confocal Optical Coherence Tomography (LC-OCT) are additional techniques providing cellular analysis of the skin in vivo [23,24], both relying on advanced AI-based image processing to extract information. Pena et al. [25] illustrated MPM's relevance for metrics such as stratum corneum/epidermis thickness and collagen density [26]. Comparatively, LC-OCT, with segmentation algorithms [27], provides micrometric data on skin layer thickness [28], quantitative cellular metrics [29], and melanin quantification [30]. Recent studies identified facial aging biomarkers using LC-OCT in different ethnicities [31,32], and Brugnot et al. characterized dermal matrix quality [33]. Deep learning models have demonstrated the potential to predict dermis age [34]. While Lupu et al. proposed the CSIESA scale based on RCM imaging [35], microscopic techniques remain scarcely part of scoring or multidimensional models. Therefore, this study adopts a multimodal approach, applying Partial Least Squares Regression (PLS2) to instrumental variables derived from LC-OCT, HFUS, Cutometer, and SkinFlex, collected from over 300 women across ethnicities. Specifically, sparse PLS (sPLS) was used to enhance interpretability by selecting the most informative predictors [36,37].

2. Materials and Methods

2.1 Study population

The study involved 328 healthy female volunteers from three ethnic groups: African-American (n = 116, mean age = 45.6 ± 14.1 years), Asian (n = 112, mean age = 44.6 ± 14.4 years), and Caucasian (n = 100, mean age = 45.5 ± 14.8 years). To ensure a balanced representation of different age categories within each population, participants were equally divided into five age groups : [20-30], [31-40], [41-50], [51-60], and [61-70] years. The Caucasian group primarily presented Fitzpatrick skin types I, II, and III; the Asian group, Fitzpatrick skin types III and IV; and the African-American group, Fitzpatrick skin types V and VI.

2.2 Skin aging measurement

a) Clinical scoring

A trained assessor conducted clinical scoring on the face to evaluate key visible signs of aging, including skin firmness (cheek, 0 to 10), density (cheek, 0 to 10), elasticity (cheek, 0 to 10), plumpness (face, 0 to 10), and crow's feet wrinkles (crow's feet, 0 to 7).The appearance of crow's feet wrinkles was assessed using a 7-point scale from 0 to 6, with intermediate grades for precision.

b) Instrumental Assessment of Skin Biomechanical Properties

The Cutometer® (Courage & Khazaka electronic GmbH, Cologne, Germany) was used to measure skin deformation by applying negative pressure. Measurements were taken on the subject's cheekbone (using a 2 mm probe) and the hollow of the cheek (using a 6 mm probe), with the side right or left randomized. Each area was measured once. All parameters derived from the Cutometer® measurements, including R0 to R9, Ue, Uv, Uf, Ur, Ua, Q0 to Q3 and F0 to F4, were recorded. [38–40]. The SkinFlex® (Orion Technolab, Tours, France) was used for non-contact measurement of the deformation under calibrated airflow [41]. Parameters computed were Maximum Depth (MD), Deformation Diameter (DD), Residual Depth (RD), firmness (inverse of the deformation volume), tension (ratio of DD to MD), and tonicity (inverse of RD).

c) Sub-Surface Imaging Techniques

Line-Filed Confocal Optical Coherence Tomogrpahy (LC-OCT) acquisitions were performed with the DeepLive™ (DAMAE MEDICAL, France) on the cheekbone, temple, and lower jawline mandible, with randomization left or right side of the face to providing 3D visualisation of skin microstructures at cellular level [27]. Studied metrics are described in [31,32]. High Frequency Ultrasounds imaging (HFUS) acquisitions were performed on the forehead, temple, and lower jawlines (mandible) with the DUB® SkinScanner (50 MHz) for the Caucasian and Afro-American subjects and the Ultrascan UC 22 (22 MHz) for Asian subjects, with the side determined by randomization. Dermis thickness, total thickness (including dermis and epidermis), dermis density, measurement of SELEB (Sub-Epidermal Low Echogenic Band) [42], as well as the depth and intensity of skin damaged were studied.

2.2 Data analysis

Statistical analysis was performed using MATLAB (MathWorks, MA, USA) as previously described [31].

Predictive models of clinical scores by multivariate analysis: Partial Least Squares 2 (PLS2) was implemented using MixOmics package in R [43]. To capture potential interactions and nonlinear relationships, first-order interaction terms (including those between phototypes and ethnic groups) were included and then transformed into four spline components using cubic natural splines. This transformation allowed the model to flexibly account for nonlinear effects, increasing the number of predictors variables. Subsequently, Sparse-PLS (L1 regularization) was used for variable selection, with phototypes and ethnic groups incorporated as dummy variables. Predictive performance was assessed through cross-validation with 25

iterations, each using different training and test sets, and evaluated using the average RMSEP (Root Mean Square Error of Prediction). This approach ensured that the model accurately captured the most relevant predictors, thereby enhancing both its robustness and predictive power.

3. Results and discussion

3.1 Clinical Scoring

Both Caucasian and Asian women exhibited significant variations in the five criteria assessed by clinical scoring with aging ($p < 0.01$), while for African-American women, variations were significant for wrinkles ($p < 0.01$), firmness ($p = 0.04$), plumpness ($p = 0.02$), and elasticity ($p = 0.01$). It was therefore confirmed that these items could be later used for the training predictive models using multivariate analysis. For wrinkles, Asian women exhibited the highest increase, with a 24.6-fold rise from the age group [20-30] (0.18 ± 0.43) to the age group [61-70] (4.94 ± 1.27). Caucasian women followed with a 15.4-fold increase from 0.16 ± 0.20 to 4.23 ± 1.26.

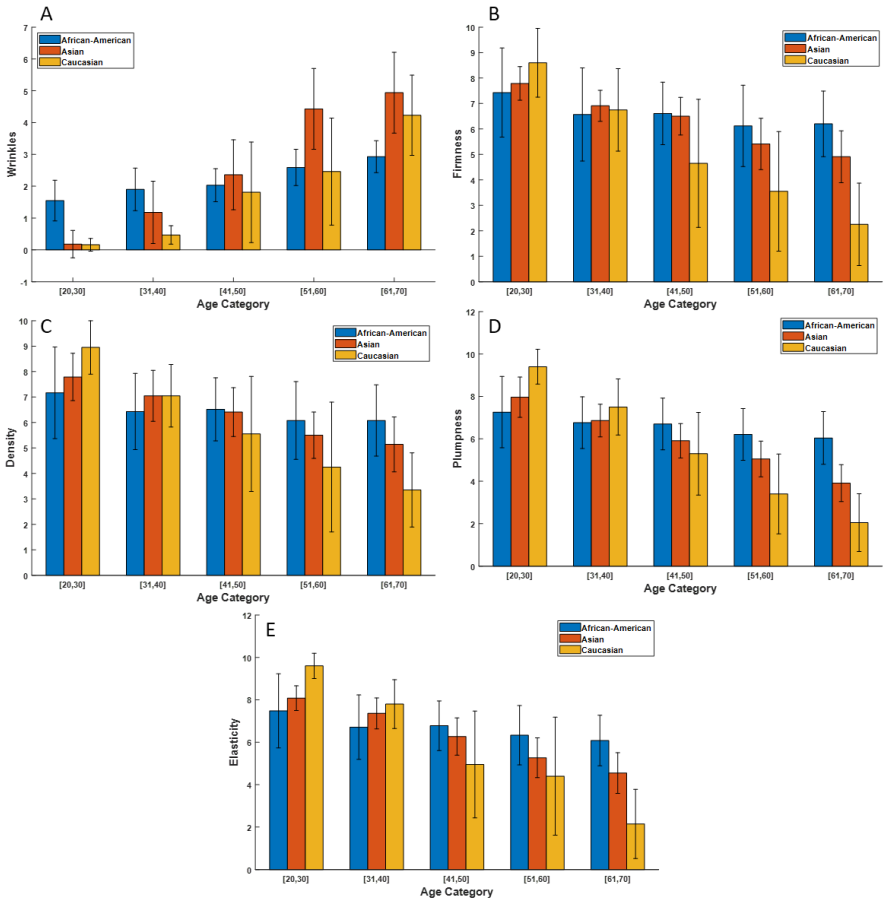

***Figure 1**. Clinical scoring performed on the African-American (Blue), Asian (Red), and Caucasian (Orange) women panels, assessing wrinkles in the "crow's feet" area (A), firmness (B), skin density (C), plumpness (D), and elasticity (E). Bars represent the mean, and error bars represent the standard deviation.*

African-American women displayed a noticeably lower increase, with a 1.9-fold rise that is significantly lower compared to both Caucasian and Asian women, with values ranging from 1.55 ± 0.64 for the younger group to 2.93 ± 0.50 for the older group. Regarding firmness, Caucasian women exhibited the most significant decrease, with a 3.8-fold reduction from the age group [20-30] (8.60 ± 1.35) to the age group [61-70] (2.25 ± 1.62). This decrease was more pronounced than the variation observed in Asian women, who showed a 1.6-fold reduction from 7.79 ± 0.66 to 4.91 ± 1.02. African-American women displayed a 1.2-fold reduction from 7.43 ± 1.75 to 6.12 ± 1.60, which is significantly lower compared to both Caucasian and Asian women. For skin density, Caucasian women exhibited the most significant decrease, with a 2.7-fold reduction from the age group [20-30] (8.95 ± 1.05) to the age group [61-70] (3.35 ± 1.46). Asian women showed a similar trend, with density decreasing from the age group [20-30] (7.79 ± 0.93) to the age group [61-70] (5.14 ± 1.08), resulting in a 1.5-fold decrease. For African-American women, the decrease was limited to a 1.2-fold reduction, from 7.43 ± 1.75 for the younger group to 6.12 ± 1.60 for the older group. For plumpness, Caucasian women exhibited the most significant decrease, with a 4.6-fold reduction from the age group [20-30] (9.40 ± 0.82) to the age group [61-70] (2.05 ± 1.36). Asian women experienced a 2.0-fold reduction from 7.96 ± 0.95 to 3.91 ± 0.87. African-American women showed a 1.2-fold reduction from 7.26 ± 1.68 to 6.04 ± 1.24, which is significantly lower compared to both Caucasian and Asian women. For elasticity, Caucasian women exhibited the most significant decrease, with a 4.5-fold reduction from the age group [20-30] (9.60 ± 0.60) to the age group [61-70] (2.15 ± 1.63). Asian women showed a more gradual decrease in elasticity, with a 1.8-fold reduction from 8.08 ± 0.58 to 4.55 ± 0.96. African-American women displayed the lowest decrease, with a 1.2-fold reduction from 7.48 ± 1.75 to 6.08 ± 1.19.

3.2 Instrumental measurements of the effects of aging

The predictive models relied on instrumental measurements of the biomechanical properties of the skin and quantifications of modifications within skin microstructures. The advantage of multivariate methods is their ability to encompass all 214 variables collected from the four techniques used to study variations with aging. Below are a few metrics used for illustration purposes.

For the Cutometer® analysis, Figures 2A and 2B illustrate age-related variations in the evolution of Q2 (elastic recovery) and R5 (net elasticity). For African-American women, both Q2 and R5 significantly and progressively decreased from the [20–30] age group (Q2 = 0.58 ± 0.15; R5 = 0.74 ± 0.19) to the [61–70] age group (Q2 = 0.44 ± 0.07; R5 = 0.62 ± 0.09). Among Asian women, Q2 and R5 showed decreases across age groups, with a significant difference observed between the youngest (Q2 = 0.52 ± 0.07; R5 = 0.69 ± 0.08) and oldest age groups (Q2 = 0.44 ± 0.06; R5 = 0.61 ± 0.09). In Caucasian women, both Q2 and R5 exhibited significant age-related reductions, particularly between the [20–30] (Q2 = 0.61 ± 0.08; R5 = 0.72 ± 0.08) and [51–60] (Q2 = 0.43 ± 0.06; R5 = 0.53 ± 0.09) age groups. Beyond this age range, no further significant changes were observed for either parameter.

For SkinFlex® analysis, Figure 2C and 2D illustrates variations in firmness and tonicity with aging. Among African-American women, firmness gradually declined, beginning in the

[31–40] (3.34 ± 1.35) and [41–50] (3.28 ± 1.32) groups, with a significant decrease in the [51–60] (2.79 ± 1.29) and [61–70] (2.24 ± 1.41) groups compared to the [20–30] group (4.48 ± 2.13). Tonicity also significantly decreased, starting in the [41–50] group (5.50 ± 2.60) and continuing through the [51–60] (4.08 ± 1.59) and [61–70] (3.35 ± 1.96) groups. For Asian women, firmness significantly declined from 3.08 ± 1.24 in the youngest group to 1.52 ± 1.19 in the oldest group, with less defined transitions in intermediate ages. Tonicity decreased from 11.06 ± 5.60 in the [20–30] group to 5.72 ± 3.42 in the [61–70] group, with reductions from [31–40] (8.29 ± 5.63) to [51–60] (4.25 ± 1.82). In Caucasian women, both firmness and tonicity showed a progressive decline across age groups. Firmness dropped from 2.36 ± 0.66 in the [20–30] group to 1.24 ± 0.25 in the [61–70] group, while tonicity decreased from 6.40 ± 2.52 to 2.22 ± 1.35 over the same age span.

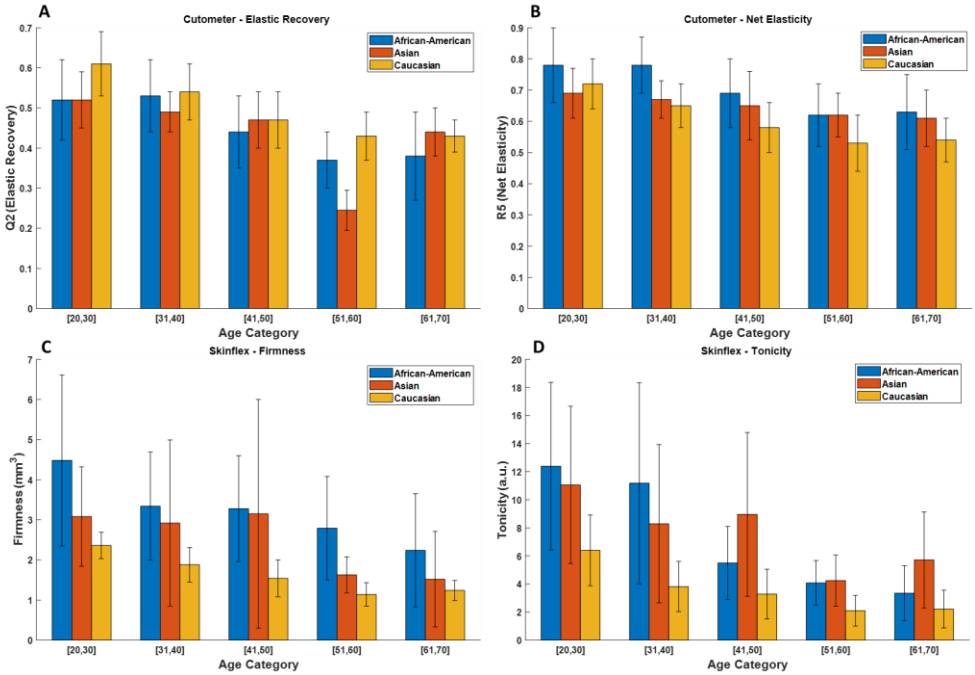

***Figure 2**. A: Q2 (elastic recovery). B: R5 (Net elasticity) measured with the Cutometer® and C: firmness. D: tonicity measured with the SkinFlex® on the African-American (Blue); Asian (Red), and Caucasian (Orange) women panels.*

For HFUS analysis (Table 1), the SELEB thickness showed a significant increase across all panels and facial areas studied, but with a higher increase observed in specific areas for each population in the Caucasian group on the forehead (from 0.0 ± 0.0 mm at age group [20–30] to 0.21 ± 0.10 mm at [61–70], $p < 0.001$), in the Asian group on the mandible (from 0.0 ± 0.01 mm at [20–30] to 0.17 ± 0.10 mm at [61–70], $p < 0.001$), and in the African-American group on the temple (from 0.0 ± 0.0 mm at [20–30] to 0.23 ± 0.23 mm at [61–70], $p < 0.001$).

Table 1: *SELEB thickness measured by HFUS*

	SELEB Thickness (mm)					
	African-American		Asian		Caucasian	
	[20,30]	[61,70]	[20,30]	[61,70]	[20,30]	[61,70]
Forehead	0.00+/-0.00 a	0.14+/-0.12 b	0.03+/-0.08 a	0.16+/-0.07 bc	0.00+/-0.00 a	0.21+/-0.10 c
Temple	0.00+/-0.00 a	0.23+/-0.23 b	0.00+/-0.00) a	0.13+/-0.07 b	0.03+/-0.07 a	0.18+/-0.10 b
Mandible	0.00+/-0.00 a	0.18+/-0.25 b	0.00+/-0.01 a	0.17+/-0.10 b	0.01+/-0.03 a	0.19+/-0.12 bc

For LC-OCT, the effects of facial skin aging in healthy Caucasian and Asian women using LC-OCT were previously reported by Bonnier et al. [31] and Assi et al. [32]. Notable age-related variations included a significant increase in SC thickness in Asian females, with the temple region increasing by 3.8% and the mandible by 5.1%. In Caucasian females, the temple showed a 7.6% increase and the mandible a 6.1% increase. In contrast, African-American females showed no significant changes in SC thickness across facial regions. For the viable epidermis (VE), Caucasian females experienced a 12.7% thinning in the mandible, with a corresponding reduction in cell layers. African-American females showed slight, non-significant reductions in cell layers in the cheekbone and mandible. Cell surface density declined significantly with age in Caucasian females' temple and mandible, and in African-American females' cheekbone and mandible. Nuclei volume increased with age across all populations, with the most variability in the mandible. In terms of nuclei compactness, Caucasian females experienced a slight decrease, while Asian and African-American females showed minimal changes. Lastly, nuclei atypia increased with age in both Asian and Caucasian females, more pronounced in the latter, while no significant changes were observed in African-American females.

3.3 predictive model of clinical signs of aging (Clinical scores)

Table 2 presents the accuracy of predictive models trained on either chronological age or clinical scores. The model predicting chronological age yielded an RMSEP of 10.10 ± 1.26 years, while the clinical score models showed RMSEP values ranging from 1.40 ± 0.12 (for wrinkles) to 1.81 ± 0.14 (for elasticity). However, these values are not directly comparable due to the differing scales of the predicted variables: chronological age spans a range from 20 to 70 years, whereas clinical scores are bounded between 0 and 10 for most scores, except for Crow’s feet wrinkles, which range from 0 to 7. Given these differences in scale and the fact that clinical scores directly reflect observable phenotypic features of the skin the present analysis specifically focused on models trained on clinical scores.

Starting with 214 initial variables, first-order interactions created 22791 new variables. These, along with the initial variables, were transformed into 5 splines, totaling 114925 variables. Interactions with ethnicity (3 categories) and phototype (6 categories) increased this to over 115000. Partial Least Squares (PLS) regression was used for dimensionality reduction,

projecting variables into a lower-dimensional space. Sparse PLS then focused on the most informative variables to improve interpretability and efficiency. Optimal hyperparameters (number of selected variables and latent components) were determined via 25-fold cross-validation, with sparse PLS models trained independently on each training subset. The combination yielding the lowest average Root Mean Square Error of Prediction (RMSEP) was selected as optimal (5000 variables, 5 components). Variable Importance in Projection (VIP) scores were calculated to visualize metric weights.The contribution of the different features are presented in figure 3. In figure 3A, the weights are presented technique-wise. Considering the sum of VIP weight LC-OCT accounts for 44% compared to HFUS (24%), cutometer (18%) and SkinFlex (15%), highlighting its predominant role in the prediction of clinical scores. This can be justified by the micrometric resolution information it provides about skin layers and quantitative cellular metrics.

Table 2: *Accuracy of models for prediction of chronological age and clinical scores. (RMSEP: Root Mean Square Error of Prediction)*

Model	Predicted Parameter	Mean_RMSEP	STD_RMSEP
Chronological Age Model	Age (Years)	10.10	1.26
Clinical Scores Model	Wrinkles	1.40	0.12
	Firmness	1.78	0.13
	Density	1.70	0.12
	Plumpness	1.61	0.11
	Elasticity	1.81	0.14

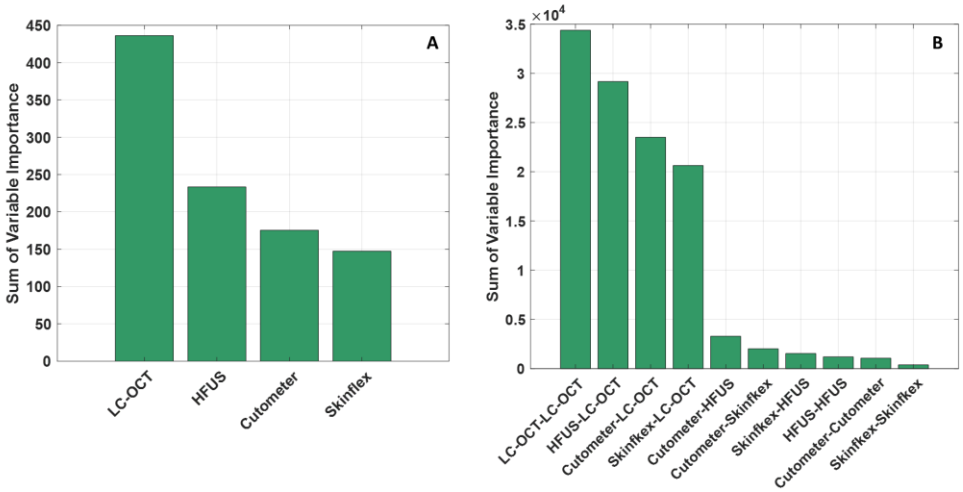

Figure 3. *A: Summed Variable Importance in Projection (VIP) scores for features derived from single-instrument features. B: Summed Variable Importance in Projection (VIP) scores for features derived from cross-instrument interactions.*

Figure 3B shows interaction-wise results. LC-OCT's contribution is highest in self-interaction (LC-OCT × LC-OCT, cumulative weight 34382), compared to interactions with HFUS (29168), Cutometer (23511), and SkinFlex (20640). Parameter-level interaction analysis identified the top 10 metric pairs with the highest VIP scores for each technique-technique interaction. For LC-OCT × LC-OCT, strong correlations existed between epidermal/stratum corneum thickness and cellular features like cell density, nuclei volume, and nuclei compactness. Interactions among cellular metrics, especially nuclei volume, nuclei compactness, and cell layer count, also significantly impacted the model. In HFUS × LC-OCT, the depth of skin damage from HFUS strongly correlated with LC-OCT cellular parameters, particularly nuclei volume and compactness. For Cutometer × LC-OCT, Cutometer metrics R6 (visco-elasticity) and R7 (immediate recovery) from the 6 mm probe, indicative of viscoelastic recovery, interacted with LC-OCT features like nuclei compactness, cell density, and cell network atypia, suggesting a link between skin's mechanical properties and microstructure. Finally, in SkinFlex × LC-OCT, SkinFlex's tonicity correlated with both cellular features (cell density, cell layer count) and histological metrics (epidermal thickness), showing how perceived firmness relates to cellular and tissue-level structures. These results demonstrate that different techniques capture complementary aspects of skin aging. Integrating them provides a deeper, more biologically relevant interpretation of age-related structural and functional changes. This pattern highlights the importance of incorporating multi-technique interactions into predictive modeling, revealing synergistic relationships often missed when using individual techniques alone, leading to a better, more comprehensive understanding.

5. Conclusion

The interplay between visible signs of aging, biomechanical properties, and modifications in skin microstructures can be challenging to establish using traditional statistical methods. Multivariate analysis enables the construction of comprehensive models encompassing hundreds of variables to highlight the correlation between perceived signs of aging and instrumental measurements through the prediction of clinical scores. Presently, allowing first-order interactions between quantitative metrics has demonstrated that associations of imaging and biomechanical properties carry a higher weight in the prediction models, emphasizing the multilevel interrelationship of parameters. Ultimately, focusing on deciphering the signs of aging through instrumental measurements opens perspectives for acquiring better knowledge of the skin aging process and supporting efficacy claims for skincare products by associating macroscopic scores with multimodal measurements, bridging the cause-effect relationship, and thus consolidating scientific evidence of efficacy.

Bibliography

[1] Vierkötter A et al. 2012;4:227–31. https://doi.org/10.4161/derm.19858.
[2] Ganceviciene R et al. 2012;4:308–19. https://doi.org/10.4161/derm.22804.
[3] Bazin R et al. Paris: Éditions Med'Com; 2007.
[4] Bazin R et al. Paris: Éditions Med'Com; 2011.
[5] Bazin R et al. Paris: Éditions Med'Com; 2013.

[6] Vierkötter A et al. 2009;53:207–11. https://doi.org/10.1016/j.jdermsci.2008.10.001.
[7] Ye R et al. 2021;20:256–62. https://doi.org/10.1111/jocd.13461.
[8] Campiche R et al. 2019;18:614–27. https://doi.org/10.1111/jocd.12806.
[9] Dicanio D et al. 2009;10:757. https://doi.org/10.1007/s10522-009-9222-6.
[10] Nkengne A et al. 2013;19:291–8. https://doi.org/10.1111/srt.12040.
[11] He Y et al. 2018;32:1060–4. https://doi.org/10.1080/13102818.2017.1423515.
[12] Pardo LM et al. 2020;182:1379–87. https://doi.org/10.1111/bjd.18523.
[13] Robic J et al. 2023;29:e13222. https://doi.org/10.1111/srt.13222.
[14] Rajadhyaksha M et al. 1999;113:293–303. https://doi.org/10.1046/j.1523-1747.1999.00690.x.
[15] Farage MA et al. 2008;30:87–95. https://doi.org/10.1111/j.1468-2494.2007.00415.x.
[16] Varani J et al. 2006;168:1861–8. https://doi.org/10.2353/ajpath.2006.051302.
[17] GILCHREST BA. 1996;135:867–75. https://doi.org/10.1046/j.1365-2133.1996.d01-1088.x.
[18] Zhang J et al. 2024;23:e14054. https://doi.org/10.1111/acel.14054.
[19] Vergilio MM et al. 2021;30:897–910. https://doi.org/10.1111/exd.14363.
[20] Vergilio MM et al. 2021;27:966–73. https://doi.org/10.1111/srt.13033.
[21] Longo C et al. 2013;68:e73–82. https://doi.org/10.1016/j.jaad.2011.08.021.
[22] Lboukili I et al. 2022;27:070902–070902. https://doi.org/10.1117/1.jbo.27.7.070902.
[23] Koehler MJ et al. 2010;16:259–64. https://doi.org/10.1111/j.1600-0846.2010.00437.x.
[24] Latriglia F et al. 2023;13:2268. https://doi.org/10.3390/life13122268.
[25] Pena A-M et al. 2022;12:14863. https://doi.org/10.1038/s41598-022-18657-z.
[26] Montgomery KL et al. 2024;14:26129. https://doi.org/10.1038/s41598-024-76908-7.
[27] Dubois A et al. 2018;23:106007–106007. https://doi.org/10.1117/1.jbo.23.10.106007.
[28] Monnier J et al. 2020;34:2914–21. https://doi.org/10.1111/jdv.16857.
[29] Chauvel-Picard J et al. 2022;15:e202100236. https://doi.org/10.1002/jbio.202100236.
[30] Jdid R et al. 2024;30:e13623. https://doi.org/10.1111/srt.13623.
[31] Bonnier F et al. 2023;13:13881. https://doi.org/10.1038/s41598-023-40340-0.
[32] Ali A et al. 2024;30. https://doi.org/10.1111/srt.13643.
[33] Breugnot J et al. 2022;29:e13221. https://doi.org/10.1111/srt.13221.
[34] Assi A et al. 2024;14:24113. https://doi.org/10.1038/s41598-024-74370-z.
[35] Lupu M et al. 2022;12:3161. https://doi.org/10.3390/diagnostics12123161.
[36] Cao K-AL et al. 2008;7:Article 35. https://doi.org/10.2202/1544-6115.1390.
[37] Cao K-AL et al. 2011;12:253. https://doi.org/10.1186/1471-2105-12-253.
[38] Ohshima H et al. 2013;19:e238–42. https://doi.org/10.1111/j.1600-0846.2012.00634.x.
[39] Dobrev H. 2005;11:120–2. https://doi.org/10.1111/j.1600-0846.2005.00090.x.
[40] Qu D et al. 2016;67:37–44.
[41] Hemmati P et al. 2022;00:1–6. https://doi.org/10.1109/bec56180.2022.9935592.
[42] Levy J et al. 2021;13:24. https://doi.org/10.1186/s13089-021-00222-w.
[43] Rohart F et al. 2017;13:e1005752. https://doi.org/10.1371/journal.pcbi.1005752.